Design of Modular Underwater Vehicle Biomimetic Hull Towards Onboard Lab-On-a-Chip Devices

Edisson A. Naula Duchi, Brian Ismael Chávez Viveros, Santiago Pérez Burciaga, Luis E. Garza-Castañón, and J. Israel Martínez-López *

Tecnológico de Monterrey, Escuela de Ingeniería y Ciencias, Monterrey, Mexico
Email: a00825462@tec.mx (E.A.N.D.), a01424135@tec.mx (B.I.C.V.), a01252991@tec.mx (S.P.B.), legarza@tec.mx (L.E.G.C.)
*Correspondence: israel.mtz@tec.mx(J.I.M.L.)

***Abstract*—The conditions for the operation of Point-of-Care sensors on water bodies are complicated to meet. The limited energy resources and footprint onboard are additional limitations of remote sensing devices. To provide a platform to perform a sufficient number of samples, the customization of Underwater Vehicles involves an integral optimization of space distribution, operation of the sensing mechanisms, and navigation. In this paper, we showcase the design and manufacturing of an Underwater Vehicle towards integration of a microfluidic device platform with a biomimetic approach. To develop this design Fusion 360 was used to sketch the internal components, including the fluid handling unit of the Lab-On-a-Chip biosensor and the reagent reservoirs, hull, and the submarine propulsion system (propeller and dorsal and pectoral fins). Furthermore, we have compared the numerical performance of three different pectoral fins for a shark, devil fish, and a drag reduction evaluating the lift and drag forces using COMSOL Multiphysics for different angles of attacks, demonstrating that a design with more cross-sectional area has 5 times greater drag and up to 3 times greater lift than a balanced and slim design. the final design will depend on the maneuverability requirements of the vehicle. The modularized design was manufactured and integrated successfully using Fusion Deposition Modelling and Stereolithography.**

***Keywords*—Point-of-Care, microdevices, hydrodynamics, hull design, UAV, Underwater vehicle, MUV, Modular Underwater Vehicle**

I. Introduction

Autonomous Underwater Vehicles (AUV) had been largely developed in recent years. These vehicles, having the capacity of completely different tasks, can be deployed in a wide variety of fields. A small-scale vehicle can provide a way to explore water bodies for environmental purposes. This complemented with sensors integrated in the vehicle, opens an area of opportunity for the investigation of Point-of-Care (POC) devices. Microfluidic devices allow to perform analysis, that normally are perform in a laboratory, on the site with advantages as less risk of contamination and reagent reduction. However, the integrations of these two fields involves an engineering and scientific challenge for each particular application. An advantage of the deployment of chemical sensors that can sample with spatial and temporal resolution data is that events and transitions in bio-geochemistry can be observed at greater detail compared than the traditional scheme of recovering samples and test them off-site [1, 2].

Microfluid enhanced devices have been incorporated recently for in-situ nitrate and phosphate analysis in the deep sea (200 m) using a LOC composed of triple layered PMMA microfluidic chip connected to an onboard syringe pump [3]. This device integrated a Dean flow mixer based on a simplified semi-circle micromixer from another research group [4] for the detection of nutrient analysis (nitrate and phosphates) at the deep sea. Research has been also conducted on more shallow water bodies. In example, another research group developed a droplet based microfluidic sensor for nitrates and nitrites for a tidal river and tested for three weeks [5]. This setup had outstanding onboard features such as integrated heater, peristaltic pump and a dual flow-cell for processing the sample.

Underwater Vehicles (UV) can be classified by their application, autonomy and the propulsion strategy used. The most common propulsion systems are propeller-based; by their autonomy, they can be autonomous, remotely operated and a point between these two. The application or task to be perform will determine the different parts or approaches in the development of an UV. However, an UV must have some basic parts: Hull, propulsion system, microcontroller board, sensors and actuators.

If a complex system, such as POC sensors, has to be integrated and it will require a higher grade of customization in the hull design which implies a complex manufacturing process. 3D printing is a process of creating three-dimensional objects by adding layers of material,

Manuscript received March 7, 2023; revised July 17, 2023; accepted August 8, 2023.

doi: 10.18178/ijmerr.12.5.324-331

such as plastic or metal one layer at a time, based on a 3D Computer-Aided Design (CAD) model. The process typically involves the use of a 3D printer. There are several different types of Additive Manufacturing (AM) processes, including Fused Deposition Modeling (FDM), Stereolithography (SLA), Selective Laser Sintering (SLS), and Electron Beam Melting (EBM), among others. This approach offers many advantages over traditional manufacturing methods, including the ability to create complex geometries and shapes that would be difficult or impossible to produce using traditional methods. It is also faster and more cost-effective for small production runs or custom products.

In this paper, we explore further the design and development of an AUV focusing on the integration with a microfluidic device for nitrite analysis (Fig. 1). Also, three different types of biomimetic pectoral fins are designed and tested (Fig. 3). The design will take into consideration parameters as energy consumption, payload, communication and time between measurements. These will define the hardware required for the functioning of the vehicle. Also, the impact on the marine environment is to be considered. The complexity of the software depends on the autonomy of the vehicle. For the manufacturing of the AUV, custom parts are build using additive manufacturing, having into account that final geometry of the vehicle will affect the hydrodynamics.

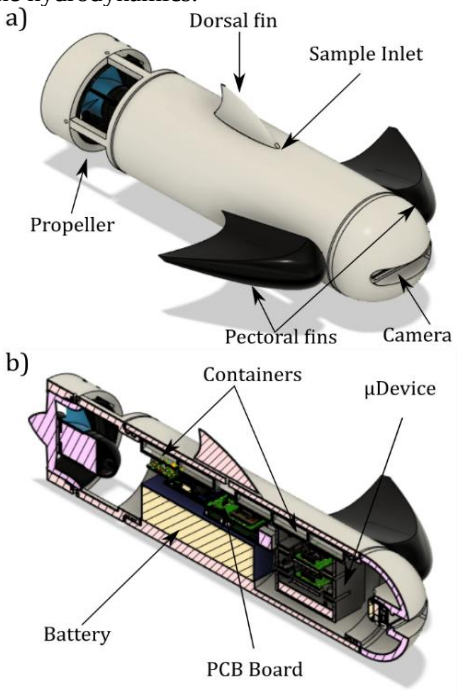

Figure 1. Proposed UAV platform. a) Structural elements. b) Inner components.

II. Literature Review

The detection of indicators of pollution, has been presented as area of opportunity for microfluidic-based technology [6]. Solutions aiming to automatize the analysis process have been presented, such is the case of a system for monitoring of phosphate and nitrite in agricultural water environments [7]. A promising approach, for quantitative assessment of environmental health risks, can be achieved with microfluidic dilution network-based devices [8]. Other approach is using colorimetry for nitrite analysis [9]. This device was the base for future version which is used for an improved phosphate blue assay and application to fluvial monitoring for long deployments [10]. There are also devices to obtain continuous in situ high temporal and spatial resolution of NO_2 *and* NO_3 measurements [11]. The automation of analitycal process will increase the data for aiding the understanding of biogeochemical cycles in the ocean [12]. These are some approaches on integration of microfluidic technology and each one has limitations according the complexity of the analysis to be perform. A recent work presented an automated phosphate analyzer that incorporated an inlaid microfluidic absorbance cell manufactured using micro milling and laser cutting and tested on an oceanic sensor platform that supports sensing instruments using a subsea cable at 100m of depth for 36 hours [13]. Another research group has effectively incorporated a spectrophotometric pH sensor to monitor hydrothermal plume underwater CO_2 release. The device was introduced previously and has a 12- cm diameter x 20 cm housing and was incorporated on a STEMM-CCS ROV Isis platform [14]. The measurements were processed on a cuvette in-situ with a 10 min time per sample. The sensor was integrated into the ROV and transmitted data in real time to the control room [15].

Modular Underwater Vehicles (MUVs) with biomimetic hulls have been an active area of research for several decades. In the early 1990s, researchers from the Massachusetts Institute of Technology mimicked the swimming mechanism of tunas using flexible body with multiple joints and an independent tail fin [16]. Since then, the method has been expanded to other species, including the approach taken by Jun Gao *et al.*, who developed a flexible biomimetic MUV with a manta ray-like shape [17], and the plethora of hulls based on shark fins and hulls [18–20]. A notable recent example is the research developed at the University of Dokuz Eylül (Turkey) where the researchers concluded that the shape of the vehicle improved the stability and efficiency under different water conditions while lowering the production cost [21].

A recent review on the combination of rigid and soft materials or components to produce novel hybrid robots [22] is a valuable resource tool for future innovations. The authors have emphasized the role of additive manufacturing in building complex, multi-material, and multifunctional systems. A classification of the use of AM technologies in soft robotics as a function of how these technologies are employed in the whole soft robot manufacturing cycle is presented in the work of [23]. The development of practical soft robotics prosthetic hands was achieved, with a focus on the ease of manufacture and functionality [24]. Furthermore, a study on the performance of a propeller for an AUV, manufactured using additive manufacturing using ABS [25]. The research provides insights into the advantages of

unconventional manufacturing technologies for complex and cost-efficiently designs.

III. Materials and Methods

A. Submarine Hull Design

The geometries are parameterized with terms as: aft body, middle body, fore body, body length, cross-section diameter, tail and nose radius. The common geometry for submarines is a torpedo-shaped geometry which was widely studied and provide benefits mechanical restraint and drag reduction, therefore it is usually used as base for more complex designs [26]. A biomimetic design offers different locomotion tactics, maneuver tactics, resistance to pressure, reduction of resistance, navigation systems and any other requirement for applications in an underwater environment with less environmental impact. Given this, we can mix these approaches to developed a design that meets the requirements for our application. Then, the parts to consider for our design are the hull, the pectoral fins for maneuverability and the propulsion system (Fig. 2a).

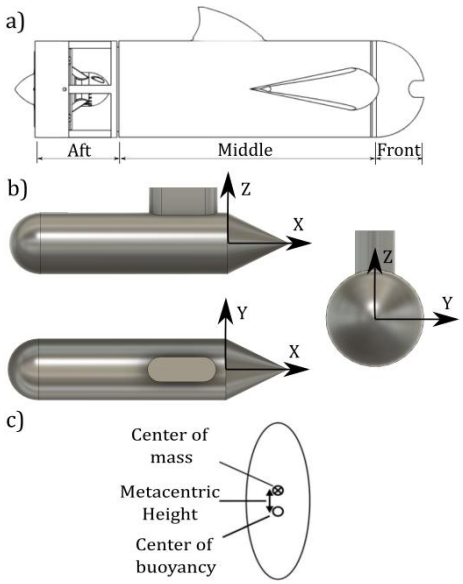

Figure 2. Basic geometry and body principles of an UV. a) Underwater vehicle parts; b) Typical geometry; c) Points of interest.

1) Hull

- Geometry: Spherical hulls offer the best structural integrity; however, the shape inhibits the efficient use of available space since most of the components and systems are rectangular. The cylindrical hulls (middle body) provide the best alternative, which includes a high structural integrity and a suitable shape for the support of electronic components. Also, the symmetry in the geometry simplifies the calculation of the center of mass and buoyancy (Fig. 2b, c).;
- Nose (Front): The nose can be used to place a camera to record images or video and for assisted navigation.;
- Aft: functions basically as a support for the propulsion system.

2) Pectoral fins

In the Thunniform locomotion of fishes the displacement is like that of a glider. The mobile pectoral fins allowed the controls of yaw and pitch movement [27]. In addition, the pectoral fins can also provide enough thrust for multimodal locomotion, such as forward swimming, spinning, descending and climbing. Hence, the profile design of the fin has a significant impact in the maneuverability of the vehicle.

In thunniform locomotion the caudal fin causes the main impulse, but pectoral fins are used to control the direction and inclination. Aiming to have a biomimetic design, three different designs inspired on dissimilar were selected for the assessment (see Fig. 3):

- The first design or design A (Fig. 3a) was inspired in a shark's fin. The design takes into account the rigidity required in the fin and the space for the motor that will provide the movement and has the profile of a crescent moon when watch it from above.
- The second design or design B (Fig. 3b) is based on the anatomy of the Hypostomus plecostomus, also called Pleco or Devil Fish, this species is native to South America but has reached Mexican lands thanks to weather events and has dominated rivers and lakes in different parts of the Mexican Republic. We take this design into account given that we aim to explore the environment that this species dominates.
- The third design or design C (Fig. 3c) aims to reduce the drag generated by the previous design and has a slender design characteristic of fish with rigid body displacement.

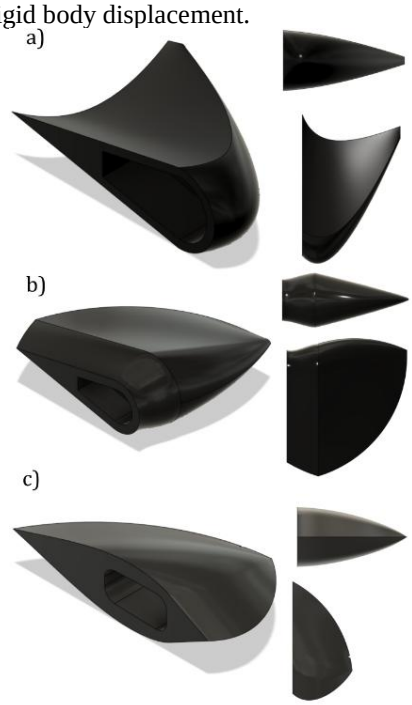

Figure 3. Biomimetic; a) Design A (shark); b) Design B (Devil Fish); c) Design C (drag reduction).

3) Propulsion

The propulsion system allows the vehicle to move in an aquatic environment. Propellers are the most common used in underwater robots and consist of an electric motor coupled to a helix that generates the thrust when displacing the fluid. Other locomotion mechanisms could be incorporated in the future considering a universal socket designed for this device.

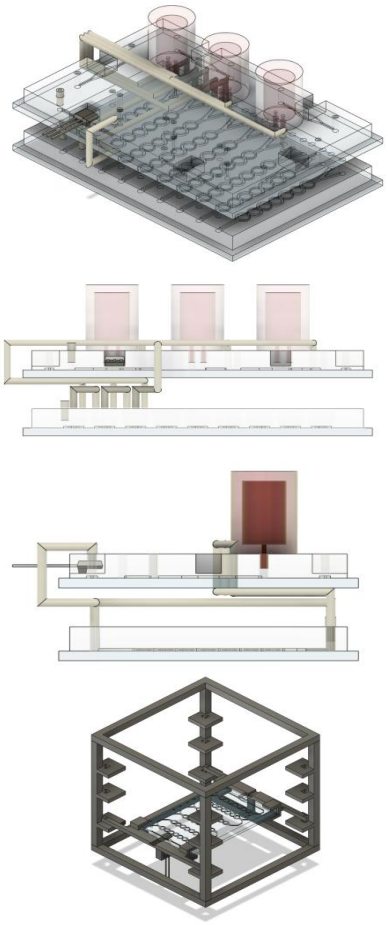

Figure 4. Modular design of a LOC device that integrates reagent reservoirs and a microdevice fixture.

4) Hardware

The hardware are the different electronic components of the vehicle. They perform tasks for navigation, communication and task related to the application of the vehicle. Some of them are:

- Energy source: the energy sources used for submarine robots include batteries, accumulators, fuel cells, among others. The batteries are composed of electro-chemical cells that store energy.
- Microcontroller board: is responsible for the main control processes of the system and the other electrical components. Depending on the autonomy it can be more complex.
- Drivers: a driver controls the operation of different devices from a control signal provided by a main Central Processing Unit (CPU). This device can handle different scales of current according the requirement of the actuator.
- Sensors: the sensors of UV depend on the activities to be carried out. They can be used to measured variables of the vehicle, acquired signal of the environment and perform the task for the application of the vehicle.
- Microdevice: in previous works [28], the study of manufacturing techniques using stereolithography for lab-on-chip (LOC) devices for their integration with autonomous vehicles was carried out. The case study was a microfluidic device for the measurement of nitrate concentration by spectrophotometry. This design was improved and modified for its future integration with a water vehicle (see Fig. 4).
- Other electronics parts are the light source and the photosensor for the spectrophotometry assay.

B. Mathematical Model

The movement of an AUV is described in two reference planes and the equations of forces that influence the vehicle. The frame of reference of an AUV has two coordinate systems: The inertial coordinate system $E-\xi\,\eta\,\zeta$ that is fixed to the Earth and the system of movement coordinates $O-xyz$ that is fixed in the vehicle. The AUV movement has six degrees of freedom (6-DOF) with three translational and three rotational movements. The general equations, of movement of the AUV, in six degrees of freedom are based on the kinetic theory of the rigid body and these are:

$$\boldsymbol{M}_{RB}\dot{\boldsymbol{v}} + \boldsymbol{C}_{RB}(\boldsymbol{\omega})\boldsymbol{v}\} = \boldsymbol{\tau}_{RB} \tag{1}$$

where $\boldsymbol{\tau}_{RB} = [\boldsymbol{F}_0^T,\ \boldsymbol{M}_0^T]^T \in \mathbb{R}^6$ is the vector of excitation forces acting on the rigid body, $\boldsymbol{v} = [\boldsymbol{u}^T,\ \boldsymbol{\omega}^T]^T = [u, v, w, p, q, r]^T \in \mathbb{R}^6$ is the velocity vector, $\boldsymbol{M}_{RB}\dot{\boldsymbol{v}}$ is the rigid body mass matrix and $\boldsymbol{C}_{RB}(\boldsymbol{\omega})$ is the Coriolis-centripetal matrix. The external forces and moments acting on the vehicle, right part of Eq. (1), are described in vector form as:

$$\tau_{RB} = F_G + F_B + F_H + F_T + F_f \tag{2}$$

where $F_G + F_B$ is the hydrostatic force acting on the vehicle due to gravity and buoyancy; F_H is a force related to the geometry of the vehicle and it includes the force of inertia and forces due to the viscosity of the fluid; F_T is the force provided by the propulsion system and F_f is the force provided by the pectoral fins.

1) Propulsion system

Force provided by the propulsion system of the AUV. In Eq. (3) describes the thrust generated by a propeller propulsion system with rotation speed n, diameter D, thrust coefficient K_T and rotation coefficient K_Q.

$$\begin{aligned} X_T &= K_T \rho\, n^2 D_b^4 \\ K_T &= K_Q \rho\, n^2 D_b^5 \\ Y_T = Z_T &= M_T = N_T \end{aligned} \tag{3}$$

2) Pectoral fins

Fins works as rudders for the AUV. When the fin has an angle of attack α (Fig. 6a), the effects can be decomposed into lift force and drag force. $F_{L_{fin}}$ and $F_{D_{fin}}$ can be calculated as:

$$\begin{cases} F_{L_{fin}} = \frac{1}{2} C_L \rho A_f u^2 \\ F_{D_{fin}} = \frac{1}{2} C_D \rho A_f u^2 \end{cases} \quad (4)$$

where C_L and C_D are the lift and drag coefficients of the fin, ρ the density of the fluid, V the velocity of the fluid and A_f the lateral area of the fin.

C. Manufacturing Process

1) Microfluidic devices

The technique for microdevices manufacture can be explained in five steps:

(1) The first step consists on additive manufacturing process based on stereolithography of photocurable resin to create a mold part with a Formlabs Form 3 equipment (Formlabs, Somerville, MA).
(2) The molds are post-processed using the recommended settings.
(3) Polydimethylsiloxane (PDMS) Sylgard 184 (Dow Corning, Midland, MI) curing agent and polymeric base are mixed in a 10: 1 proportion and then poured to the assembled mold.
(4) The PDMS is cured in hot plate and detached from the mold using manual tools (knife and tweezers).
(5) The removed PDMS slab and a microscope glass slide are then introduced in an Expanded Plasma Cleaner (Harrick Plasma, Ithaca, NY) for surface treatment which activates the PDMS surface for glass bonding.

These steps are performed for each module. More details on the manufacture process are shown in [28].

2) Hull, fins and supports

AM technologies offer a way to produce 3D objects with tool-less processes and complex geometries. The Fuse Filament Fabrication (FFF) process, which is also call FDM, uses thermoplastics as matrix that is extruded through a nozzle in patters and creating successive layers formed by filament roads. Step motors are used to control the horizontal plane (x-y) of the nozzle and the vertical movement (z) can be achieved either by also moving the nozzle or by moving the platform. The material is fed to the liquefier by gears.

This technique was used to fabricate the hull of the vehicle (middle body), the supports for the propulsion system (aft body), the nose of the vehicle (front body) and the pectoral fins of the vehicle (Fig. 3a). Also, the internal supports for the microfluidic device (Fig. 4) where manufactured by this method.

D. Integration of the Microdevice

The integration implies dealing with some limitations, such as energy management, ship impermeability, payload management and measurement frequency. Furthermore, considering the turbidity found in natural water bodies, a filtering phase for the sample is required. The filter must be able to prevent the passage of particles larger than the width of the microchannels (200 μm) to avoid clogging the circuit. As seen in Fig. 5, the filter can be attached at the entrance of the sample inlet and can also be built with AM. The fluid handling also has an important role in maintaining the equilibrium of the vehicle, this is because the center of mass can be affected by the instantaneous position of the fluid mass during specific moments during the mission. The internal fluid on the microdevice is about 0.18 mL, so it can be considered irrelevant in order to change the center of mass. However, the container for each reagent and for the waste have a capacity of 5 mL each, so in order to avoid changes because of this, the containers are placed along the symmetry line of the vehicle, as shown in Fig. 1b. Following this concept, the tubing and also other components must be placed and secured trying to maintain symmetry to avoid unnecessary displacements in the center of mass.

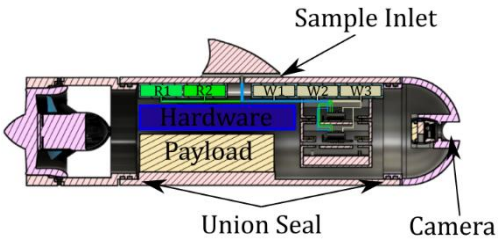

Figure 5. Proposed UAV platform integration with microdevice.

Assuring the impermeability of the vehicle underwater is another crucial challenge to consider during the design and manufacturing process. The critical regions to consider as a source of leaking are the unions between sections of the vehicle and the sample inlet for the microfluidic device. A cavity connecting to the vehicle's exterior should be available during sampling. One alternative to achieve this is employing a valve at the aperture. However, another more straightforward solution is implementing a syringe pump that withstands the pressure and only draws the fluid when required for water characterization. Thereby, a customized syringe pump has been placed inside the hull. The device will drag the sample and the reagents whenever required by the microcontroller.

E. Computational Fluid Dynamics

COMSOL Laminar Flow module was used to simulate the interaction of three different pectoral fins with three-dimensional models generated. The fins were considered as a solid, and the domain surrounding the fin was set as a fluid domain of water ($\rho = 1000\ \mathrm{kg/m^3}$). The straight-line test simulates a tunnel where the AUV or the fins can be placed and the flow has constant velocity. In this test the linear and angular acceleration are zero. Here, the solid is located under a given angle respect to the flow direction and there is no pitch movement ($q = 0$). Different types of movements can be simulated by placing the body in different planes. The resulting force estimated, in the side plane position (Fig. 6a), its divided into Lift (F_L) and Drag (F_D) forces that are perpendicular and parallel to the flow

velocity. The applied force perpendicular to the longitudinal axis is calculated by:

$$Z = F_D \sin\alpha + F_L \cos\alpha \quad (5)$$

Multiple simulations with α within -15 and 15 can be performed to have an estimation on the drag and lift force generated for each design of pectoral fin.

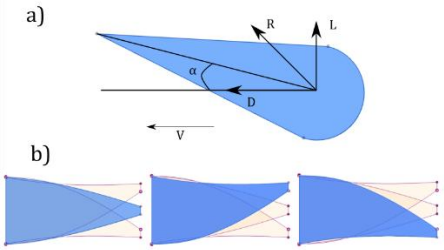

Figure 6. a) Right side profile; b) Front profile with α as 0, 10 and −10 degrees of inclination.

IV. Result and Discussion

All the parts mentioned above can be assembled to obtain the prototype shown in Fig. 7. The middle body, nose, and supports were fabricated on a Fortus 400mc printer (Stratasys, Rehovot, Israel) with polycarbonate-ISO (PC-ISO) material. Acrylic was used to seal the hole in the front camera and in the rear part at the joint with the supports of the propulsion system. The three parts of the body were sealed by embedded flanges and with the use of O-rings for waterproofing. In the dorsal fin there is a hole to allow hoses bring water samples from outside the hull into the microfluidic device. On the sides there are notches to place the servomotors that will move the pectoral fins.

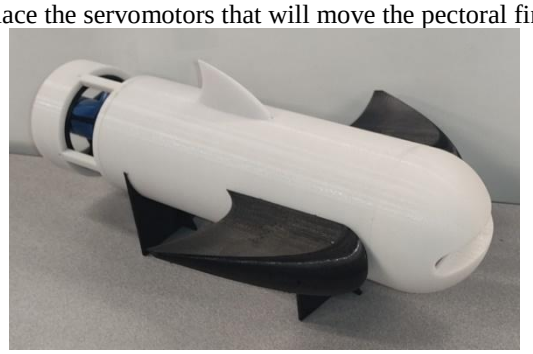

Figure 7. Photograph of the final prototype manufactured with additive manufacturing and mounted pectoral fins Design A type.

A. Manufacturing of Fin Prototypes

The fins were manufactured with a process similar to that of the helmet, but with the difference that an Ender 5 PRO (Creality, Shenzhen, China) was used with polylactic acid (PLA) filament. The motors are embedded both in the body of the vehicle and in the fin itself. The result can be seen in Fig. 8.

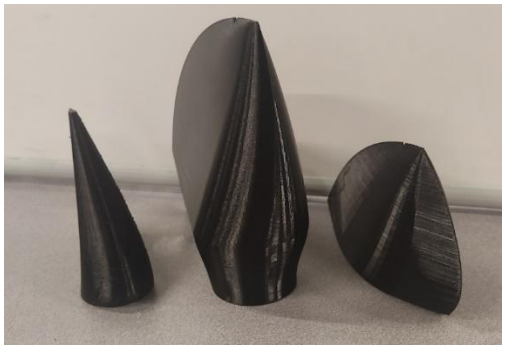

Figure 8. Photograph of biomimetics fins manufactured with additive manufacturing.

From a manufacturing point of view, making vehicle parts using AD facilitates the customization of the parts; although, depending on the manufacturing method, the cost can be higher, and the manufacturing time can also increase significantly. An example of this is if we make the fins by FDM, its manufacture takes around 14 hours, while using stereolithography the same design can take twice as long. The difference in the results lays on the resolution that can be obtained from each one, being the last one the one with the highest resolution; For this reason, it is advisable to use this method when it is necessary and for pieces that require details with a high resolution. In the case of the pectoral fins the FDM method is the most efficient.

B. Numerical Simulations

To evaluate the produced designs in terms of the hydrodynamic performance, we inspected the behavior of the pectoral fins under a varying angle of attack. The average velocity of the fluid was set in 5 m/s

1) Drag and lift estimation

COMSOL software allow to estimate the drag and lift generated on the solid, this case the fin, which can be used to have an idea on the effect that the geometry of the fin has on the hydrodynamics of the vehicle. Also, the drag and lift coefficients could be estimate instead and then we can use Eq. (4) to implement this effect on the general model of the vehicle. In Fig. 9, we can see the fluid interaction with the profile of the 3 fins under different angles of attack. Fig. 9a shows that the first design does not generate vortex around the fin, which is not the case of the second design, that generates a lot of vortexes that could disrupt the navigation and the environment. These vortexes decrease when the fin is moved to a higher angle of attack. The third design shows, as was intended, less disruption on the water and therefore is less invasive to the environment; however, when the fin has $\alpha = 15$, we can see the generation of vortex under the fin. All these simulations are only with positive α and thanks to the symmetry of the designs, the results for negative α will be the same amplitude but with opposite sign.

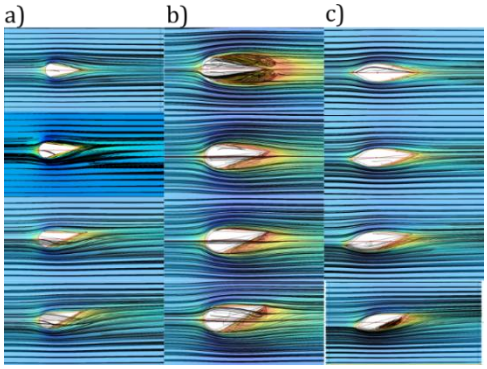

Figure 9. Fluid behavior in the calculation domain for an angle of attack, $\alpha = [0°, 5°, 10°, 15°]$ for, a) Design A; b) Design B and c) Design C.

The estimated drag and lift forces are shown in Table I and plotted in Fig. 10. The results shown that Design A and C have a similar result in lift generated, but as expected the drag generated by the design C is lower than design A. In the other hand, design B generates a much higher drag and lift than other designs. This could be due to the transversal area that is opposed to the fluid when the fin has a bigger angle of attack. However, when $\alpha = \pm 5$ the, the lift generated is opposite to the expected value, so this should be considered for implementing a control strategy. Likewise, the generation of vortices and turbulence must be taken into account, since the general design of the vehicle does not include a classic rudder and this could generate undesired forces.

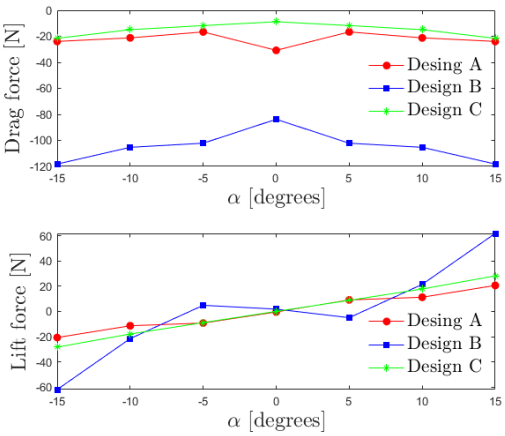

Figure 10. Estimated values of Drag force and Lift force.

TABLE I. ESTIMATED DRAG AND LIFT [N].

	α	Design A	Design B	Design C
Drag	15 °	−23.943	−118.2	−21.559
	10 °	−21.204	−105.33	−14.903
	5 °	−16.631	−102.18	−11.755
	0 °	−30.778	−83.793	−8.8112
Lift	15 °	20.65	61.886	28.263
	10 °	11.315	21.502	17.842
	5 °	9.1638	−4.901	8.8304
	0 °	-0.35763	1.8724	0.084

V. CONCLUSION

This work shows the design and development of an AUV focused on the integration with a LOC device. The approach applied is to have a bio-inspired design that will have a less impact in the aquatic environment.

Additive manufacturing allows to have a personalized AUV design which cover the needs for a specific task such as monitoring water bodies for pollution indicators. Microfluidic devices open a wide range of possibilities of automated analytic tests, that are usually perform in a laboratory, to be done in the site with advantages promoted by the size of the device and having less complexity on the logistics of the process. All of these come at the cost of complexity on the design of the vehicle, but this can be minimized by the advantages of the additive manufacturing approaches.

As shown in the results of drag and lift estimation, an agreement must be reached between the impact of the geometry and the hardware requirements to minimize or take advantage of the hydrodynamic effects that can be generated by having different bio-inspired designs.

Future work efforts will be focused on the development of the water sampling system. These additions will imply additional auxiliary systems such as filtration systems to avoid clogging. Hence, all these further experimental evaluations of energy consumption and waste management will be considered during immersion tests.

CONFLICT OF INTEREST

The authors declare no conflict of interest.

AUTHOR CONTRIBUTIONS

J. Israel Martínez and Luis E. Garza-Castañón conceptualized the research goals and aims and supervised the project operation and funding; Edisson Naula, Brian Ismael Chávez, and Santiago Pérez Burciaga conducted the research for designing and manufacturing the pectoral fins; Edisson Naula developed the Computational Fluid Dynamics and wrote the original draft; J. Israel Martínez López reviewed and edited the manuscript.

ACKNOWLEDGMENT

The authors acknowledge the financial support from the University of Ottawa-Tecnológico de Monterrey Seed Grant Program toward this research, as well as CONACyT (México) for the support given to students at Tecnológico de Monterrey through the scholarships program.

REFERENCES

[1] M. Mowlem *et al.*, "Industry partnership: Lab on chip chemical sensor technology for ocean observing," *Front. Mar. Sci.*, vol. 8, no. October, pp. 30–35, 2021, doi: 10.3389/fmars.2021.697611.

[2] B. Jiang, Z. Xu, S. Yang, Y. Chen, and Q. Ren, "Profile autonomous underwater vehicle system for offshore surveys," *Sensors*, vol. 23, no. 7, p. 3722, Apr. 2023, doi: 10.3390/s23073722.

[3] A. D. Beaton *et al.*, "Lab-on-chip for in situ analysis of nutrients in the deep sea," *ACS Sensors*, vol. 7, no. 1, pp. 89–98, 2022, doi: 10.1021/acssensors.1c01685.

[4] A. Al-Halhouli, A. Alshare, M. Mohsen, M. Matar, A. Dietzel, and

S. Büttgenbach, "Passive micromixers with interlocking semi-circle and omega-shaped modules: Experiments and simulations," *Micromachines*, vol. 6, no. 7, pp. 953–968, 2015, doi: 10.3390/mi6070953.

[5] A. M. Nightingale *et al.*, "A droplet microfluidic-based sensor for simultaneous in situ monitoring of nitrate and nitrite in natural waters," *Environ. Sci. Technol.*, vol. 53, no. 16, pp. 9677–9685, 2019, doi: 10.1021/acs.est.9b01032.

[6] M. Hamon, J. Dai, S. Jambovane, and J. W. Hong, "Microfluidic systems for marine biotechnology," *Hb25_Springer Handbook of Marine Biotechnology*, Berlin, Heidelberg: Springer Berlin Heidelberg, 2015, pp. 509–530.

[7] B. Lin, J. Xu, K. Lin, M. Li, and M. Lu, "Low-cost automatic sensor for in situ colorimetric detection of phosphate and nitrite in agricultural water," *ACS Sensors*, vol. 3, no. 12, pp. 2541–2549, 2018, doi: 10.1021/acssensors.8b00781.

[8] G. Zheng *et al.*, "Development of microfluidic dilution network-based system for lab-on-a-chip microalgal bioassays," *Anal. Chem.*, vol. 90, no. 22, pp. 13280–13289, 2018, doi: 10.1021/acs.analchem.8b02597.

[9] A. D. Beaton *et al.*, "Lab-on-chip measurement of nitrate and nitrite for in situ analysis of natural waters," *Environ. Sci. Technol.*, vol. 46, no. 17, pp. 9548–9556, 2012, doi: 10.1021/es300419u.

[10] G. S. Clinton-Bailey *et al.*, "A lab-on-chip analyzer for in situ measurement of soluble reactive phosphate: Improved phosphate blue assay and application to fluvial monitoring," *Environ. Sci. Technol.*, vol. 51, no. 17, pp. 9989–9995, 2017, doi: 10.1021/acs.est.7b01581.

[11] A. G. Vincent *et al.*, "Nitrate drawdown during a shelf sea spring bloom revealed using a novel microfluidic in situ chemical sensor deployed within an autonomous underwater glider," *Mar. Chem.*, vol. 205, pp. 29–36, 2018, doi: 10.1016/j.marchem.2018.07.005.

[12] A. J. Birchill *et al.*, "Realistic measurement uncertainties for marine macronutrient measurements conducted using gas segmented flow and Lab-on-Chip techniques," *Talanta*, vol. 200, no. March, pp. 228–235, 2019, doi: 10.1016/j.talanta.2019.03.032.

[13] S. Morgan, E. Luy, A. Furlong, and V. Sieben, "A submersible phosphate analyzer for marine environments based on inlaid microfluidics," *Anal. Methods*, vol. 14, no. 1, pp. 22–33, 2022, doi: 10.1039/d1ay01876k.

[14] S. A. Monk *et al.*, "Detecting and mapping a CO_2 plume with novel autonomous pH sensors on an underwater vehicle," *Int. J. Greenh. Gas Control*, vol. 112, no. December 2020, p. 103477, 2021, doi: 10.1016/j.ijggc.2021.103477.

[15] V. M. C. Rérolle, C. F. A. Floquet, M. C. Mowlem, D. P. Connelly, E. P. Achterberg, and R. R. G. J. Bellerby, "Seawater-pH measurements for ocean-acidification observations," *TrAC - Trends Anal. Chem.*, vol. 40, no. 0, pp. 146–157, 2012, doi: 10.1016/j.trac.2012.07.016.

[16] R. W. Smith and J. A. Wright, "Simulation of robotuna fluid dynamics using a new incompressible ale method," in *Proc. 34th AIAA Fluid Dyn. Conf. Exhib.*, 2004, doi: 10.2514/6.2004-2347.

[17] G. Jun, B. Shusheng, X. Yicun, and L. Cong, "Development and design of a robotic Manta Ray featuring flexible pectoral fins," in *Proc. 2007 IEEE Int. Conf. Robot. Biomimetics, ROBIO*, pp. 519–523, 2007, doi: 10.1109/ROBIO.2007.4522216/REFERENCES.

[18] S. Janardhanan *et al.*, "Towards the development of a bio-inspired shark-shaped unmanned underwater vehicle," in *Proc. Sustain. Dev. Innov. Mar. Technol. 18th Int. Congr. Int. Marit. Assoc. Mediterr. IMAM 2019*, pp. 240–246, Aug. 2020, doi: 10.1201/9780367810085-31/towards-development-bio-inspired-shark-shaped-unmanned-underwater-vehicle-janardhanan-venu-shahabudheen-issac-abhijith-das-ilieva.

[19] A. Raj and A. Thakur, "Fish-inspired robots: design, sensing, actuation, and autonomy—a review of research," *Bioinspir. Biomim.*, vol. 11, no. 3, p. 031001, Apr. 2016, doi: 10.1088/1748-3190/11/3/031001.

[20] M. Wright, Q. Xiao, S. Dai, M. Post, H. Yue, and B. Sarkar, "Design and development of modular magnetic bio-inspired autonomous underwater robot–MMBAUV," *Ocean Eng.*, vol. 273, p. 113968, Apr. 2023, doi: 10.1016/J.OCEANENG.2023.113968.

[21] K. T. GÜRSEL and M. Taner, "Comparison study of biomimicry-inspired forms of autonomous underwater vehicles," *SSRN Electron. J.*, 2023, doi: 10.2139/SSRN.4379642.

[22] S. Li, H. Bai, R. F. Shepherd, and H. Zhao, "Bio-inspired design and additive manufacturing of soft materials, machines, robots, and haptic interfaces," *Angew. Chemie - Int. Ed.*, vol. 58, no. 33, pp. 11182–11204, 2019, doi: 10.1002/anie.201813402.

[23] G. Stano and G. Percoco, "Additive manufacturing aimed to soft robots fabrication: A review," *Extrem. Mech. Lett.*, vol. 42, p. 101079, 2021, doi: 10.1016/j.eml.2020.101079.

[24] A. Mohammadi *et al.*, "A practical 3D-printed soft robotic prosthetic hand with multi-articulating capabilities," *PLoS One*, vol. 15, no. 5, pp. 1–23, 2020, doi: 10.1371/journal.pone.0232766.

[25] H. M. T. Khaleed, I. A. Badruddin, A. N. Saquib, M. F. Addas, S. Kamangar, and T. M. Yunus Khan, "Novel approach to manufacture an AUV propeller by additive manufacturing and error analysis," *Appl. Sci.*, vol. 9, no. 20, 2019, doi: 10.3390/app9204413.

[26] M. Renilson, "Introduction," in *Submarine Hydrodynamics*, Cham: Springer International Publishing, 2018, pp. 1–11.

[27] Z. Wu, J. Yu, J. Yuan, M. Tan, and J. Zhang, "Mechatronic design and implementation of a novel gliding robotic dolphin," in *Proc. 2015 IEEE International Conference on Robotics and Biomimetics (ROBIO)*, 2015, pp. 267–272.

[28] E. A. Naula, B. L. Rodríguez, L. E. Garza-Castañon, and J. I. Martínez-López, "Manufacturing of stereolithography enabled soft tools for point of care micromixing and sensing chambers for underwater vehicles," *Procedia Manuf.*, vol. 53, pp. 443–449, 2021, doi: 10.1016/j.promfg.2021.06.047.